

Elasto-Plastic Finite Element Analysis of Horse-Shoe Tunnels

by

R. K. Srivastava*

K. G. Sharma**

A. Varadarajan***

Introduction

Horse-shoe shaped section of underground openings is used in hydroelectric projects, highway and railway networks and in several other cases. In case of deep tunnels where the rock behaviour is in plastic range and sequence of excavation has significant effect over the final stresses and displacements developed around an underground excavation, the shape of the opening is also one of the important factors to be considered. Depending upon the shape, sequence of excavation and insitu stress ratio, tensile stresses may also develop in the surrounding rock and this may prove to be of critical importance for the stability of the underground opening.

Elasto-plastic finite element analysis of circular tunnels excavated in single and two stages for three insitu-stress ratios ($K_0 = 0.5, 1.0$ and 1.5) has been presented recently by Srivastava *et al.* (1986). In the present study, to bring out the effect of different shapes of opening, a horseshoe tunnel section has been chosen. The maximum height and width of the section is 8 m. The cross sectional area of this section is approximately 4 per cent more than that of a circular tunnel of 8 m diameter. The three insitu stress ratios for which studies have been carried out are $K_0 = 0.5, 1.0$ and 1.5 . The horse-shoe tunnel has been simulated to be excavated in single stage and in two stages. Hoek-Brown yield criterion (Hoek and Brown, 1980) has been used for the elasto-plastic analysis. The deformed shape, displacement paths and principal stresses have been presented for elastic and elasto-plastic analyses.

* Reader, Department of Civil Engineering, M.N.R. Engineering College, Allahabad-211004, India.

** Associate Professor } Department of Civil Engineering,
*** Professor } Indian Institute of Technology, Hauz Khas,
New Delhi-110016, India.

(The revised paper was received in January, 1986 and is open for discussion till the end of June, 1987)

Elasto-Viscoplasticity

The state of stress at a point is represented by the stress vector $\{\sigma\}$, ($\{\sigma\}^T = [\sigma_x \ \sigma_y \ \sigma_z \ \tau_{xy} \ \tau_{yz} \ \tau_{zx}]$) and total strain by the vector $\{\epsilon\}$, ($\{\epsilon\}^T = [\epsilon_x \ \epsilon_y \ \epsilon_z \ \gamma_{xy} \ \gamma_{yz} \ \gamma_{zx}]$).

The total strain at a point is the sum of elastic and viscoplastic strains, i.e.

$$\{\epsilon\} = \{\epsilon^e\} + \{\epsilon^{vp}\} \quad \dots(1)$$

where $\{\epsilon^e\}$ and $\{\epsilon^{vp}\}$ are the elastic and viscoplastic strain vectors, respectively.

The stresses are related to the total and viscoplastic strains through the relation

$$\{\sigma\} = [D] (\{\epsilon\} - \{\epsilon^{vp}\}) \quad \dots(2)$$

where $[D]$ is the elasticity matrix. The elements of $[D]$ are function of Young's modulus and Poisson's ratio.

The yield function, in general, can be written in the form (Zienkiewicz and Corneau, 1974)

$$F = F(\{\sigma\}, \{\epsilon^{vp}\}) = 0 \quad \dots(3)$$

Equation (3) represents in general the conditions of plasticity, hardening/softening at a point. The viscoplastic strain rates are given by the flow rule

$$\{\dot{\epsilon}^{vp}\} = \mu \langle F \rangle \frac{\partial F}{\partial \{\sigma\}} \quad \dots(4)$$

in which $\{\dot{\epsilon}^{vp}\}$ is the viscoplastic strain rate vector, μ is the fluidity parameter (taken as 1 for elasto-plastic analysis), $\langle \rangle$ is used to indicate that if $F \leq 0$, $\langle F \rangle = 0$ and if $F > 0$, $\langle F \rangle = F$.

Yield or Failure Criterion

The empirical failure criterion as proposed by Hoek and Brown (1980) is given by

$$\sigma_1 = \sigma_3 + (m \sigma_3 \sigma_c + s \sigma_c^2)^{1/2} \quad \dots(5)$$

where σ_1 and σ_3 are major and minor principal stresses, respectively, σ_c is the uniaxial compressive strength of the intact rock material and m and s are dimensionless empirical constants.

Equation 5 can be written in the form

$$F = \sigma_1 - \sigma_3 - (m \sigma_c \sigma_3 + s \sigma_c^2)^{1/2} = 0 \quad \dots(6)$$

which is applicable to perfectly plastic material. For $F \leq 0$, original rock mass is linear elastic and when $F > 0$, the rock mass starts yielding.

Computer Program

A computer program has been developed on ICL 2960 for elasto-viscoplastic finite element analysis for plane strain condition. Elasto-viscoplasticity has been used as an artifice to obtain elasto-plastic solution. The formulation adopted is as proposed by Zienkiewicz and Cormeau (1974). Eight-noded isoparametric elements and 2×2 Gauss point integration rule have been used.

The procedure adopted to simulate excavation is that proposed by Chandrasekaran and King (1974). The elements which cover the area to be excavated are made AIR elements, i.e. their contribution to the global stiffness matrix is reduced to almost zero. This is done by reducing the Young's modulus of the elements to be excavated to about 10^{-6} th of the original value. For the present study, the tunnel is simulated to be excavated in single stage (i.e. full face) and in two stages (above the springing level in the first stage and the remaining portion of the tunnel below the springing level in the second stage).

Cases Analysed

The horse-shoe tunnel section is shown in Fig. 1. The maximum height and width of the section is 8 m and is located at a depth of 250 m

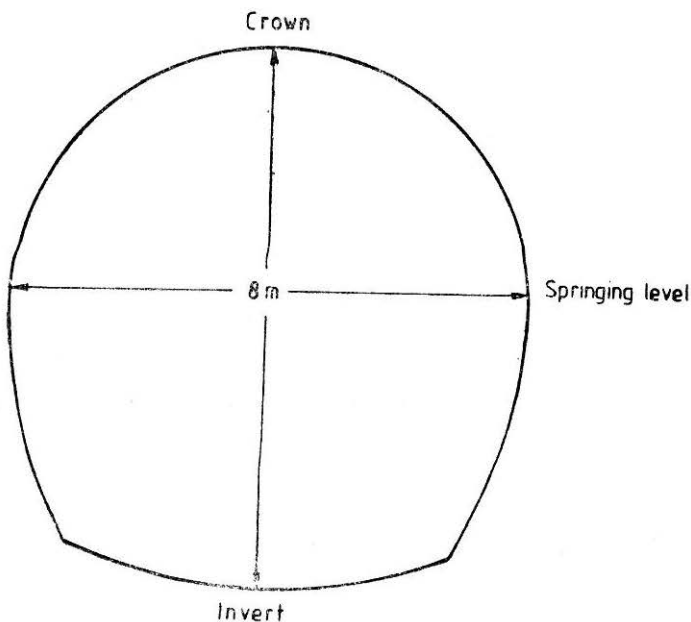


FIGURE 1 Horse—Shoe Tunnel Section

from the ground surface. Three insitu stress ratios ($K_0 = 0.5, 1.0$ and 1.5) have been considered. For each insitu stress ratio, the tunnel is simulated to be excavated in single stage and then in two stages. The rock properties used in the analyses are from a river valley project in India and are as follows:

Rock type	= Good quality Basalt
Young's modulus	= $3.5 \times 10^6 \text{ t/m}^2$
Poisson's ratio	= 0.21
Unconfined compressive strength	= 12236.4 t/m^2
Tensile strength	= 24.47 t/m^2
Insitu stress σ_v	= 675.0 t/m^2
$m = 1.7, s = 0.004.$	

In Fig. 2, the various cases analysed are shown and explained schematically.

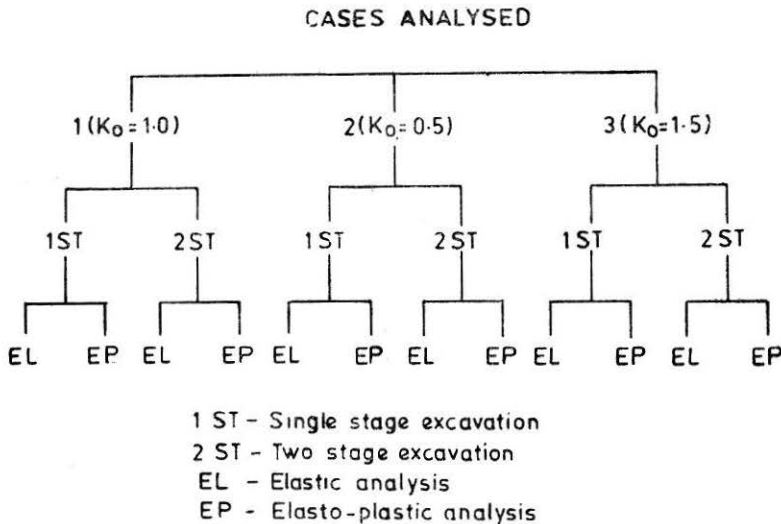


FIGURE 2 Schematic Diagram Indicating Cases Analysed

Analysis

For this shape of tunnel, several finite element discretizations have been tried and the mesh chosen is as shown in Fig. 3, keeping in view the accuracy and economy of the analysis as the criteria. Because of the symmetry of the excavation, only half horse-shoe tunnel has been analysed. For this discretization, a total number of 92 elements and 307 nodes have been used.

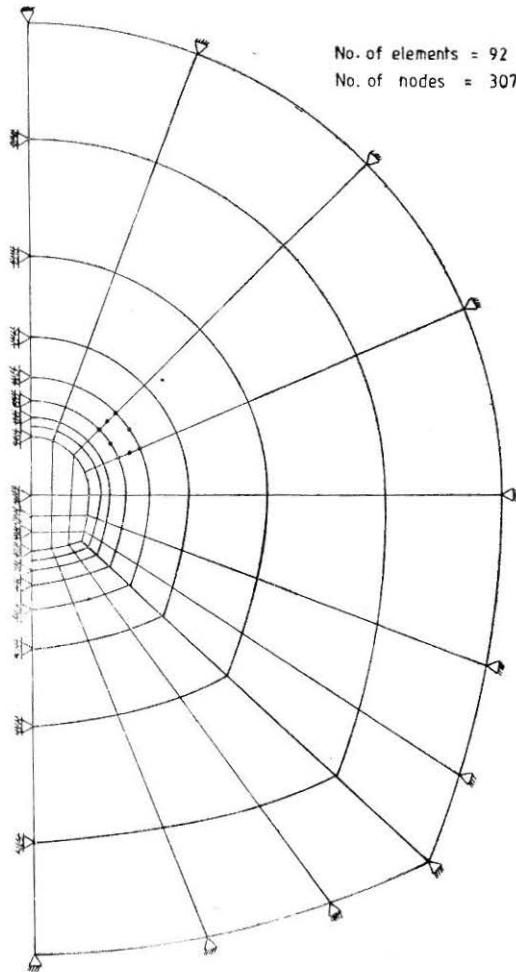


FIGURE 3 Finite Element Discretization Mesh (Half Horse—Shoe Tunnel)

Results and Discussion

Case 1 ($K_o = 1.0$)

The elastic and elasto-plastic deformed shapes of the tunnel are shown in Fig. 4. For case 1ST, the deformed shape for the elastic and elasto-plastic analyses are almost same as the tunnel shape. For case 2ST, for elastic analysis, the deformed shape after the final stage of excavation is same as for case 1ST, as expected, but for elasto-plastic analysis the final deformed shape is non-uniform.

A comparison of the displacements obtained from elasto-plastic analysis for case 1ST shows that near the springing, the displacements are slightly higher in case 1ST but at other locations, the displacements are higher in case 2ST.

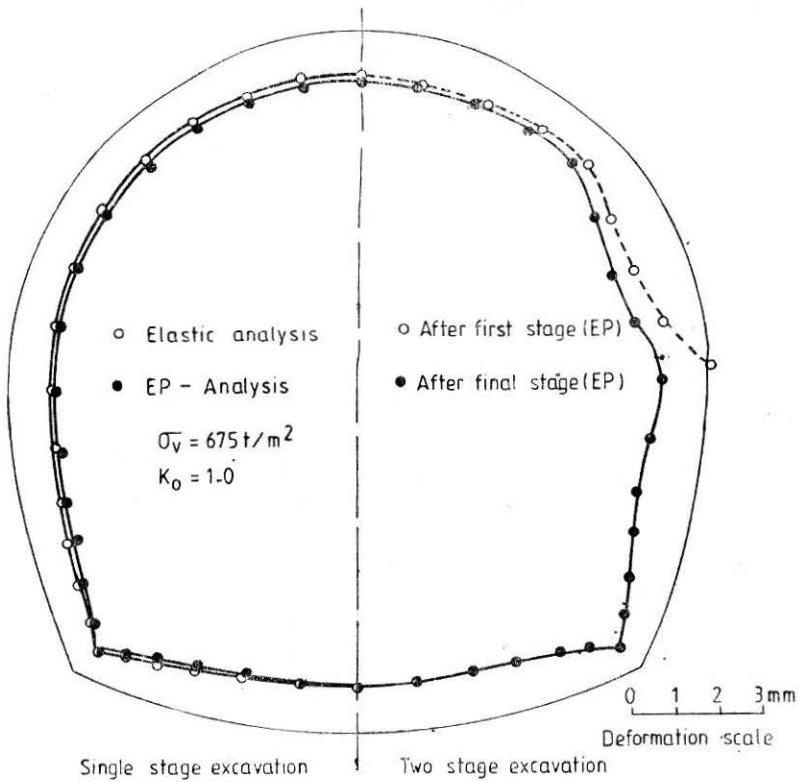


FIGURE 4 Deformed Shape of Tunnel $K_0=1.0$

The displacement paths (for elasto-plastic analysis) for four typical locations on the tunnel boundary have been shown in Fig. 5 for the two cases. The displacement paths show the movement of points at the tunnel boundary from initial to final displaced position in case 1ST and from initial to first stage displacement to final stage displacement in case 2ST. From the figure it is seen that at location 1, the movement of point is, in general, downwards and to the left but there is a marked difference in the final magnitude and direction of the movement in the two cases. At location 2, displacement path is very much different in the two cases. In case 1ST, it is to the left but in case 2ST, first the point moves upwards and to the right and then sharply to the left. However, the final magnitude of the displacement is almost same for both the cases. At location 3, below the springing level, there is appreciable difference between the direction and magnitude of the displacement of the point. In general, the movement is upwards and to the left. At location 4 in the invert portion of the tunnel, the magnitude and direction of movement are almost same. The movement is in upward direction (about 30° from vertical) and to the left.

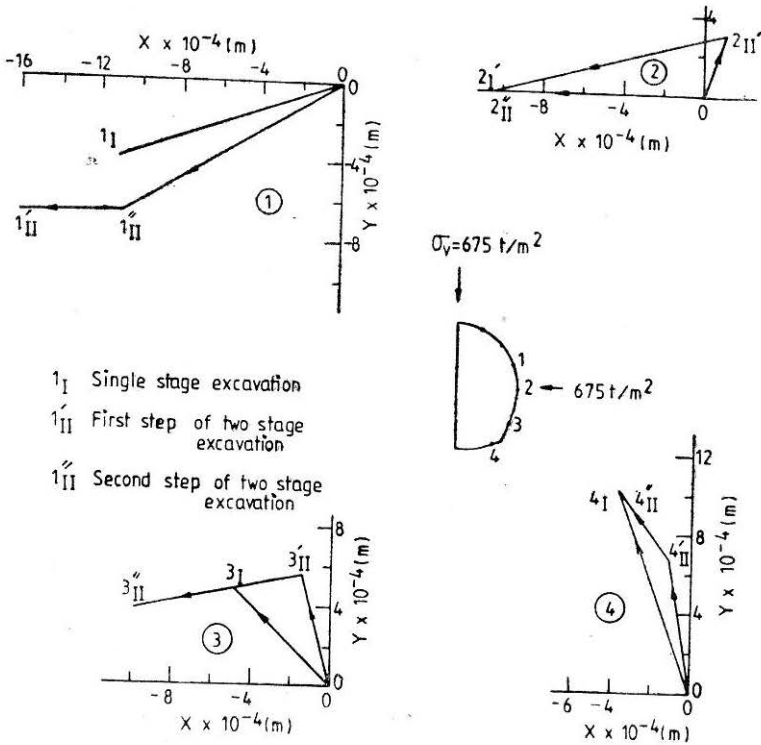


FIGURE 5 Displacement Paths—EP Analysis ($K_0=1.0$)

The major and minor principal stress contours for both the cases are shown in Figs. 6 to 8. For case 2ST, stress contours for elasto-plastic analysis only are shown. The contours, in general, clearly show the stress concentration zone near the bottom corner of the tunnel. A comparison of the stress contours for the two cases shows that both the principal stresses are significantly affected by the yielding of the rock and it is very much pronounced in case of minor principal stress.

On comparison of elastic and elasto-plastic principal stresses for case 1ST, it is seen that close to the tunnel boundary, whereas above the springing level, the minor principal stress is less, in case of elasto-plastic analysis, below the springing level of tunnel, it is greater and the maximum difference is observed in the side wall portion of the tunnel (198.9 percent). The major principal stress obtained from elasto-plastic analysis are smaller at all the locations as compared to those obtained from elastic analysis and the maximum difference observed is about 19.3 percent (in the side wall portion of the tunnel).

The maximum value of tensile stress indicated after first stage of excavation in case 2ST is near springing level and it is -199.7 t/m^2 . This is

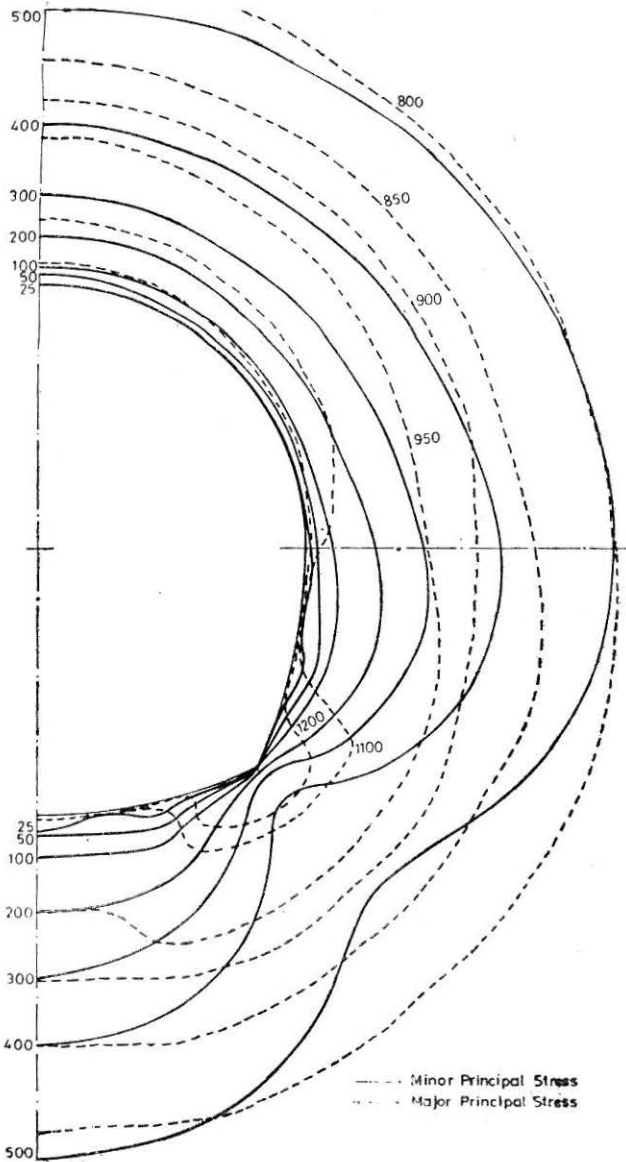


FIGURE 6 Principal Stress Contours—EL Analysis ($K_0=1.0$)

reduced to 2.5 t/m^2 (compressive) in the elasto-plastic solution obtained after completion of first stage excavation and becomes 4.1 t/m^2 after the elasto-plastic solution of the final stage of excavation is obtained.

The displacements and stresses obtained for single stage and two stage excavations for $K_0 = 1$ condition for some typical points near the tunnel boundary are presented in Table 1.

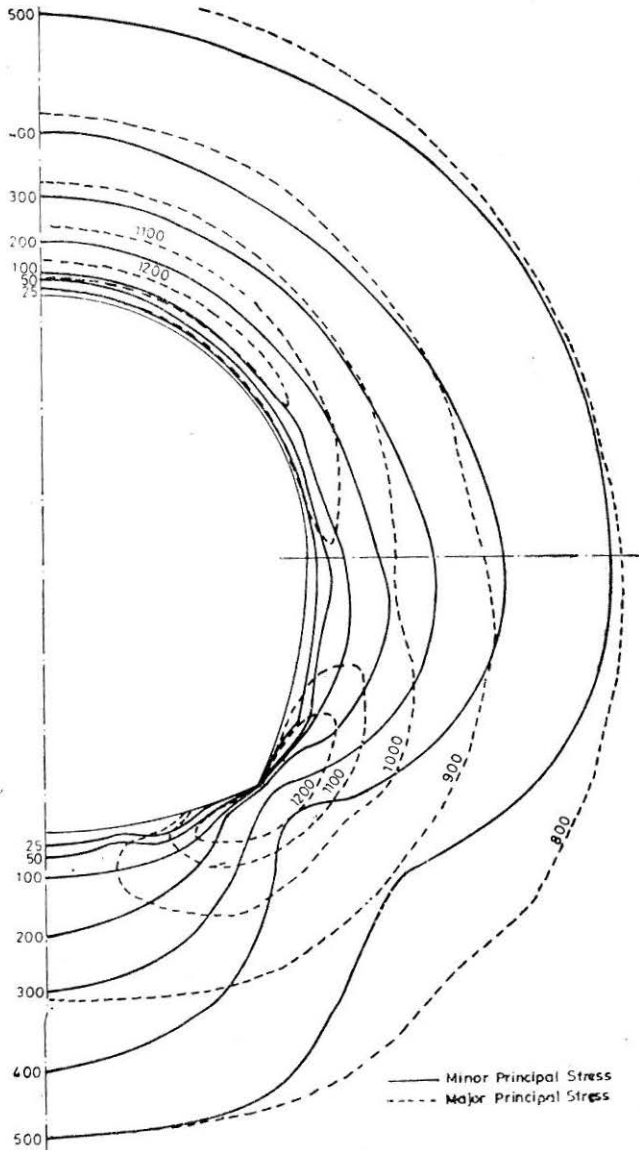


FIGURE 7 Principal Stress Contours—EP Analysis ($K_0 = 1.0$)

Case 2 ($K_0 = 0.5$)

The elastic and elasto-plastic deformed shapes of the tunnel are shown in Fig. 9. For case 1ST, the elastic deformations are higher at the crown and invert portion of the tunnel as compared to the deformations in the side wall portion of the tunnel. The elasto-plastic deformations are more in the side wall portion of the tunnel as compared to deformations in the crown or invert portion. For case 2ST the elasto-plastic deformed shape is non-uniform.

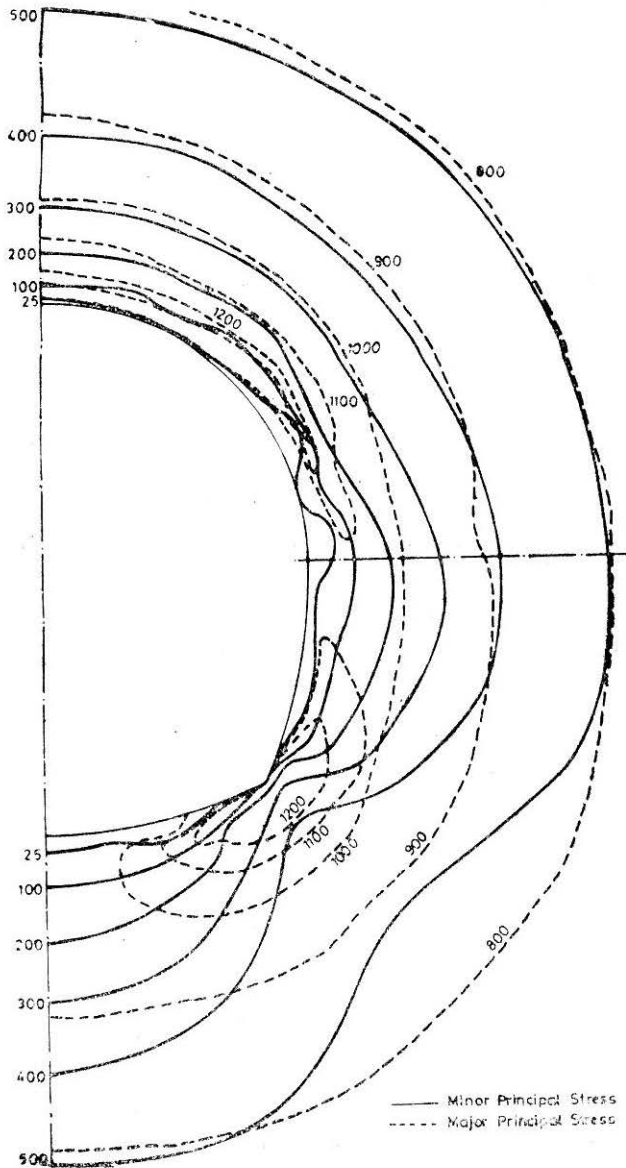


FIGURE 8 Principal Stress Contours, Two Stage Excavation—EP Analysis ($K_0=1.0$)

Comparing the displacements obtained from elasto-plastic analysis for case 2ST and case 1ST, it is found that above the springing level, the displacements are higher in case 2ST (maximum about 83.1 percent) but around springing level they are lower in this case and then again are slightly higher than case 1ST. In the invert portion of the tunnel, the difference is almost negligible.

TABLE I
Stresses and Displacements near Tunnel Boundary ($K_0 = 1.0$)

Location	Single stage excavation			Two stage excavation		Remarks
	EL	EP	Percentage difference between EP and EL	EP	Percentage difference between two stage and single stage excavation	
Resultant displacement $\times 10^{-2}$ m	1	0.095	0.109	14.81	0.175	59.56
	2	0.098	0.108	9.65	0.103	-4.70
	3	0.086	0.102	20.77	0.105	2.44
	4	0.088	0.105	18.96	0.106	0.98
Minor principal stress t/m^2	1	30.35	28.14	7.84	6.46	-77.01
	2	-10.53	10.65	-198.86	-0.29	-102.71
	3	39.29	40.59	-3.2	40.83	0.58
Major principal stress t/m^2	1	1270.5	1134.2	12.01	821.1	-38.13
	2	1086.8	910.8	19.32	758.8	-20.03
	3	1368.9	1263.0	8.38	1259.4	-0.28

EL—elastic analysis

EP—elasto-plastic analysis

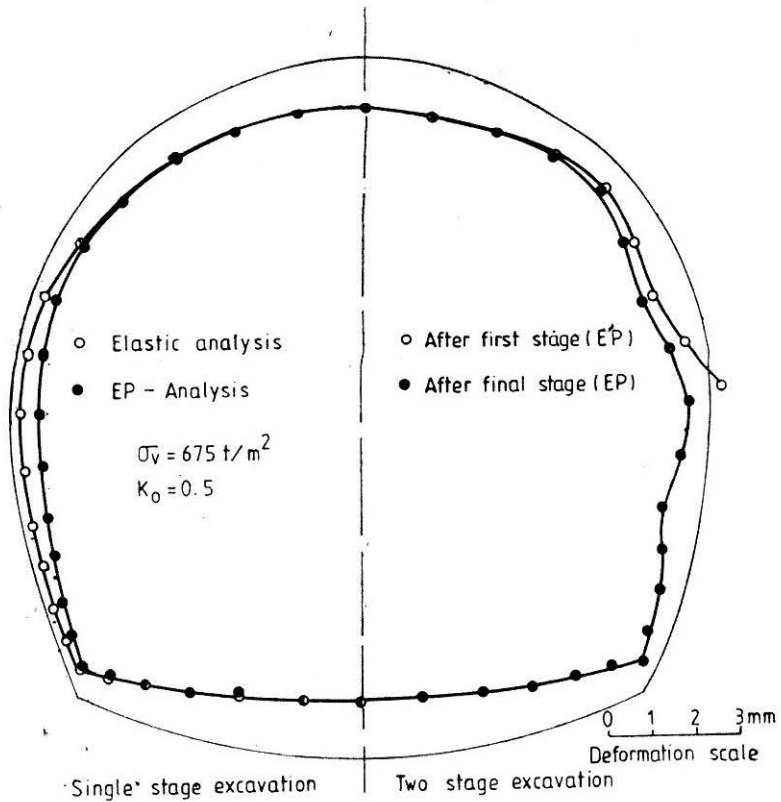


FIGURE 9 Deformed Shape of Tunnel ($K_0=0.5$)

The displacement paths (for elasto-plastic analysis) for four typical locations on the tunnel boundary are shown in Fig. 10 for the two cases. From the figure, it is seen that at location 1, the movement of the point is, in general, downwards and to the left. There is not much difference in the direction of the movement but there is marked difference in the magnitude of the displacements. At location 2, the displacement paths are very much different for the two cases. In case 1ST, it is to the left and slightly downwards but in case 2ST, first the point moves upwards and to the right and then sharply to the left. There is slight difference in the magnitudes of the final displaced position. At location 3, the final direction and magnitude are almost same. The final direction is to the left and about 45° upwards. At location 4, in the invert portion of the tunnel, the magnitude and direction are same for the two cases and it is almost in the vertical direction.

The major and minor principal stress contours are shown in Figs. 11 to 13, for both the cases. For case 1ST stress contours are shown for both elastic and elasto-plastic analyses, whereas for case 2ST, stress contours for only elasto-plastic analysis are shown. The contours, in general,

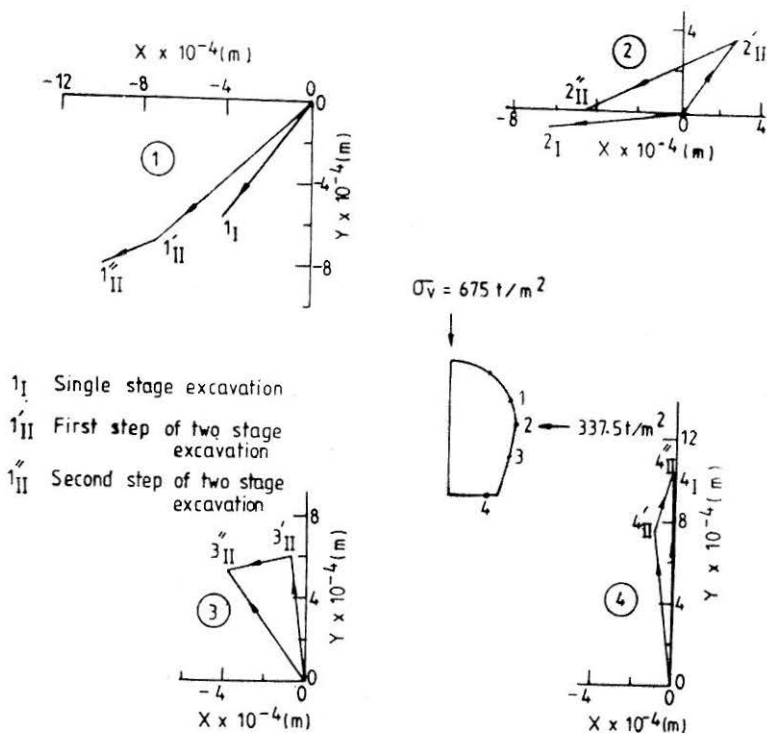


FIGURE 10 Displacement Paths—EP Analysis ($K_0=0.5$)

show the stress concentration zone near the bottom corner of the tunnel. A comparison of stress contours for the two cases shows that both the principal stresses are affected by yielding of the rock and the effect is more pronounced in case of minor principal stress in this case.

A comparison of elastic and elasto-plastic stresses for case 1ST shows that the maximum difference occurs in the side wall portion of the tunnel. It is observed that at few locations close to the tunnel boundary, the minor principal stresses are higher for elasto-plastic analysis in the side wall portion of the tunnel as compared to those obtained from elastic analysis however, the values involved are very small. The major principal stresses obtained from the elasto-plastic analysis are less than those obtained from elastic analysis and the maximum difference observed is in the side wall portion (about 35.4 percent).

The maximum value of tensile stress indicated after the first stage of excavation in case 2ST is near the springing level of the tunnel and it is $111.4 t/m^2$. This is reduced to $12.6 t/m^2$ (compressive) in the elasto-plastic solution obtained after completion of the first stage excavation and becomes $6.3 t/m^2$ (compressive) after the elasto-plastic solution of the final stage excavation is obtained.

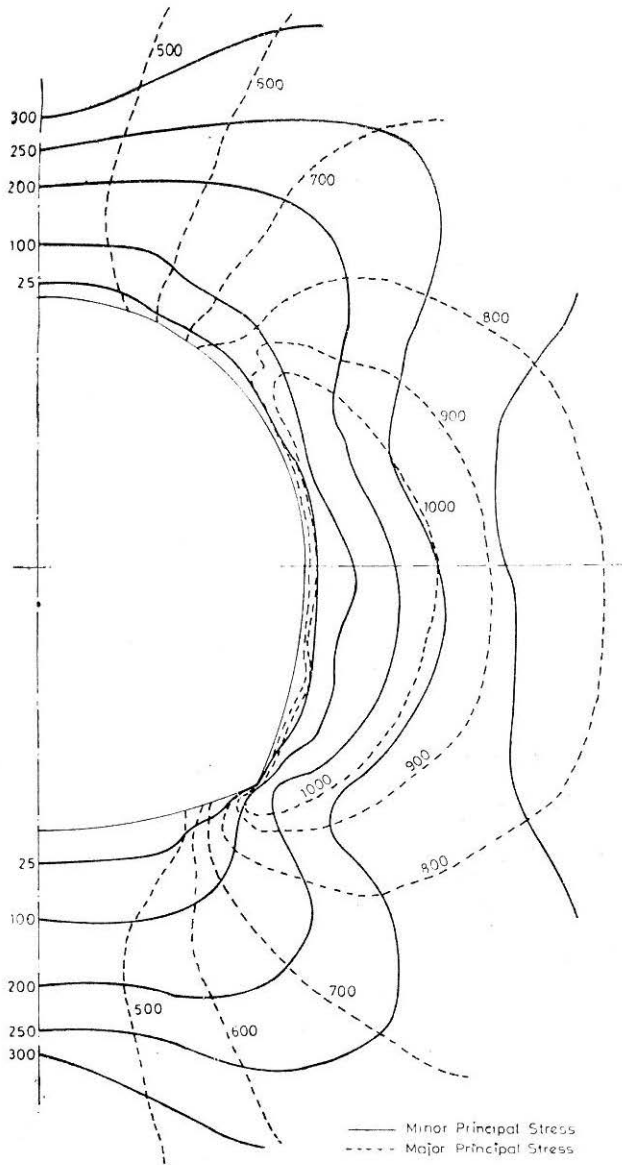


FIGURE 11 Principal Stress Contours—EL Analysis $K_0=0.5$

In Table 2 are presented the displacements and stresses obtained for case 1ST and case 2ST for some typical locations near the tunnel boundary.

Case 3 ($K_0 = 1.5$)

The elastic and elasto-plastic deformed shapes of the tunnel are shown in Fig. 14. For case 1ST, the elastic deformations are higher near the

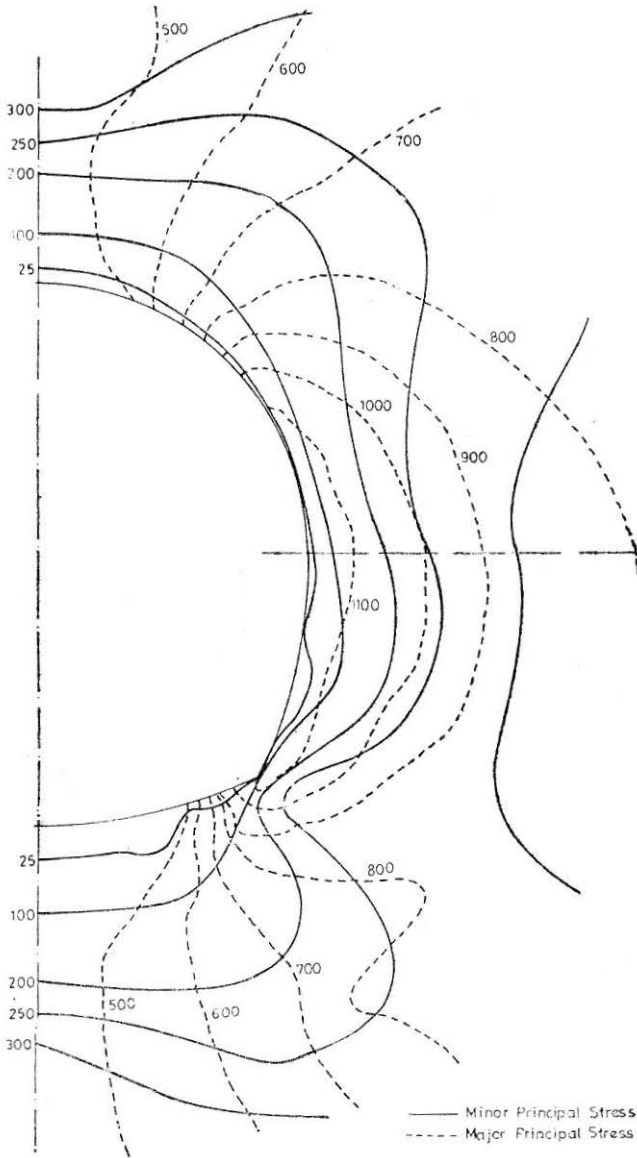


FIGURE 12 Principal Stress Contours—EP Analysis ($K_0=0.5$)

springing level of the tunnel and smaller in the crown and invert portions of the tunnel. The elasto-plastic deformations are more in the crown and invert portions of the tunnel and in the side wall portion, they are smaller. For case 2ST, the elasto-plastic analysis indicates large deformations in the side wall of the tunnel in the second stage of excavation (the solution does not converge and comparatively large deformations are indicated). As such, the deformed shape indicates comparatively unstable tunnel.

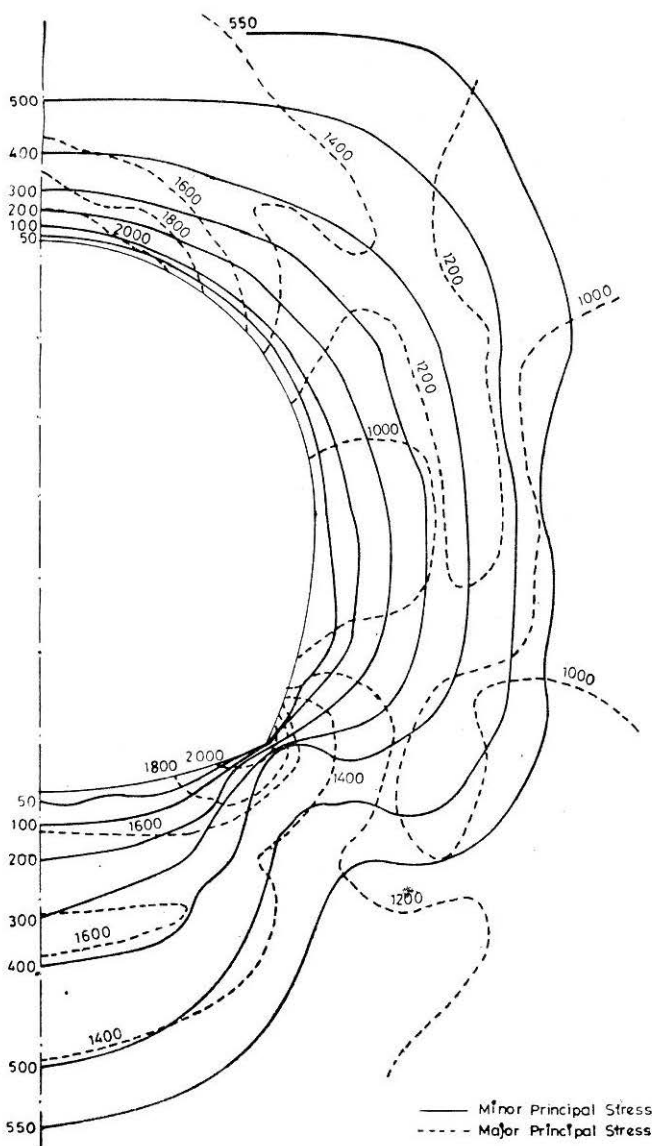


FIGURE 13 Principal Stress Contours, Two Stage Excavation,—EP Analysis ($K_0=0.5$)

Considering case 1ST, large differences are found in the displacements at the tunnel boundary between elasto-plastic and elastic analyses at the crown and invert of the tunnel. The difference around springing level is negligible. For the present set of properties, elastic displacements at the crown of the tunnel is $0.652 \times 10^{-3} m$; at the springing level of the tunnel is $0.169 \times 10^{-2} m$ and at the invert of the tunnel is $0.879 \times 10^{-3} m$. The maximum difference observed between elasto-plastic and elastic analyses is about 168 percent near the crown of the tunnel.

TABLE 2
Stresses and Displacements Near Tunnel Boundary ($K_0 = 0.5$)

Location	Single stage excavation			Two stage excavation		Remarks
	EL	EP	Percentage difference between EP and EL	EP	Percentage difference between two stage and single stage excavation	
Resultant displacement $\times 10^{-3}$ m	1	0.515	0.704	36.76	1.289	83.07
	2	0.280	0.649	131.99	3.471	-27.51
	3	0.491	0.634	29.09	0.661	4.21
	4	0.994	1.013	1.94	1.020	0.70
Minor principal stress t/m^2	1	27.4	26.9	1.75	39.2	45.50
	2	0.1	12.9	Large	1.67	-86.90
	3	3.0	-0.1	104.4	0.81	703.50
Major principal stress t/m^2	1	1285.8	1116.2	15.19	771.6	-30.87
	2	1267.6	936.2	35.39	816.2	-12.81
	3	720.3	712.67	1.06	712.43	-0.03

EL—elastic analysis

EP—elasto plastic analysis

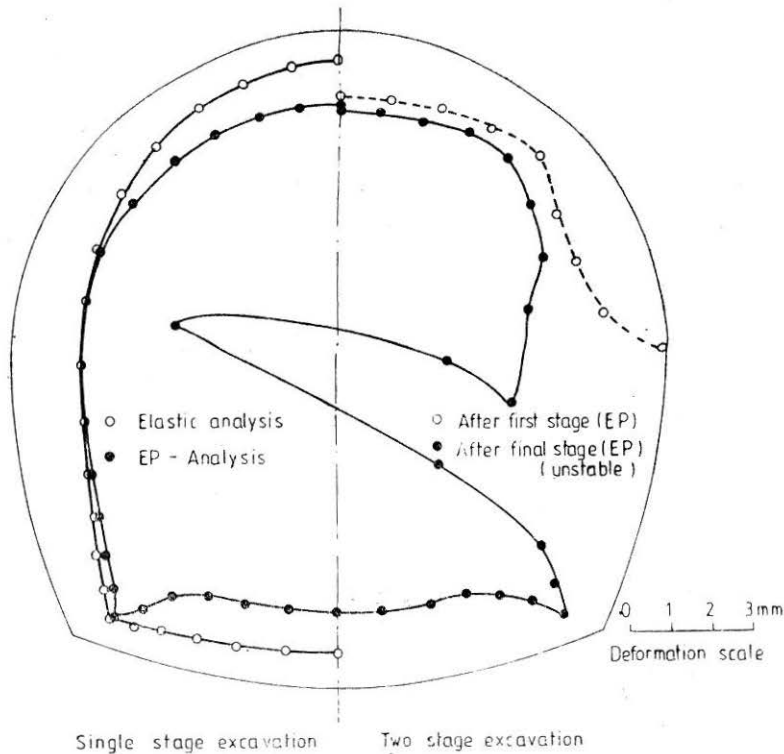


FIGURE 14 Deformed Shape of Tunnel ($K_o = 1.5$)

The displacements obtained in case 2ST from the elasto-plastic analysis (non-converged solution) are very large in the side wall portion as compared to case 1ST. The maximum difference between the two stage excavation and single stage excavation is about 616.3 per cent in the side wall portion of the tunnel.

The displacement paths (for elasto-plastic analysis only) for five typical locations on the tunnel boundary are shown in Fig. 15 for both the cases. From the figure it is seen that at location 1, the movement of the point is, in general, to the left and downwards. There is marginal difference in the direction of movement and marked difference in the magnitudes of displacements in the two cases at location 1. At location 2, in general, the movement is towards the left. For case 2ST, it is first slightly downwards and then to the left. At location 1, for case 1ST, the movement is towards the left and slightly upwards, while for case 2ST, the movement is upwards and to the left. This location clearly indicates large magnitude of deformation as compared to case 1ST. At location 3, the movement is towards the left and upward. There is marginal difference in the final magnitudes of displacements in the two cases. At location 4, the movement is

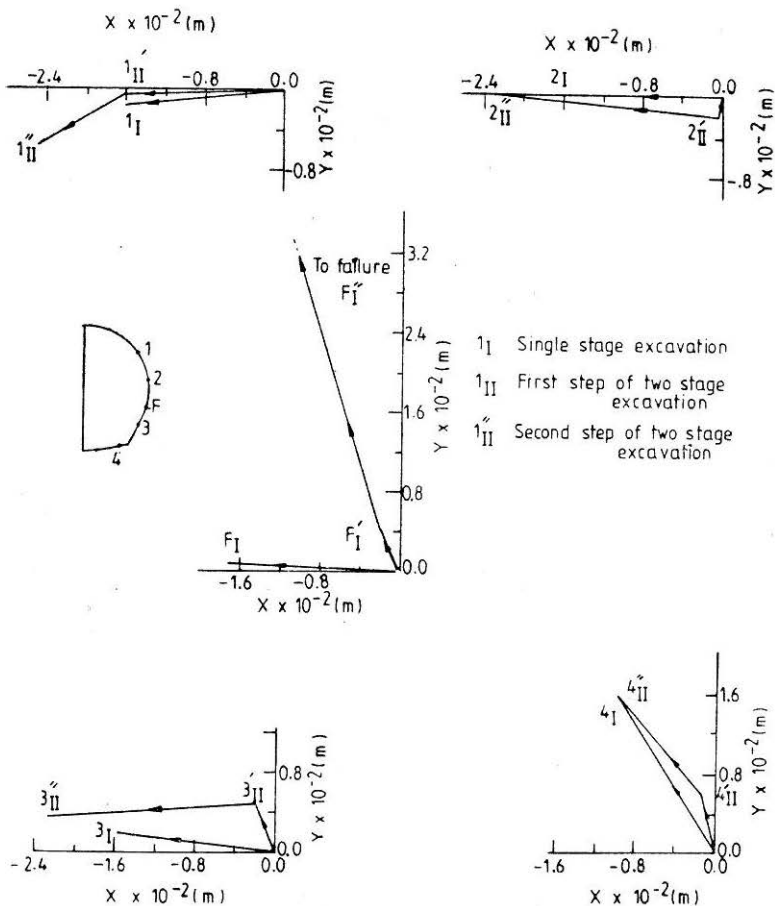


FIGURE 15 Displacement Paths—EP Analysis ($K_o = 1.5$)

upwards and to the left (about 45°). The final magnitude and direction are almost same in the two cases at this location.

The major and minor principal stress contours are shown in Figs. 16 and 17 for case 1ST (for both elastic and elasto-plastic analyses). For case 2ST, since the elasto-plastic analysis indicates a comparative instability of side walls, hence the principal stress contours are not shown. The contours, in general, show the stress concentration zone near the bottom corner of the tunnel. A comparison of stress contours for the elastic and elasto-plastic analyses shows that both the principal stresses are affected by yielding of the rock and it is more pronounced in the case of major principal stresses.

The maximum value of tensile stress indicated for this insitu stress ratio in case 2ST, after the first stage excavation is also near the springing level and it is -299.6 t/m^2 . This is reduced to -5.7 t/m^2 after the first

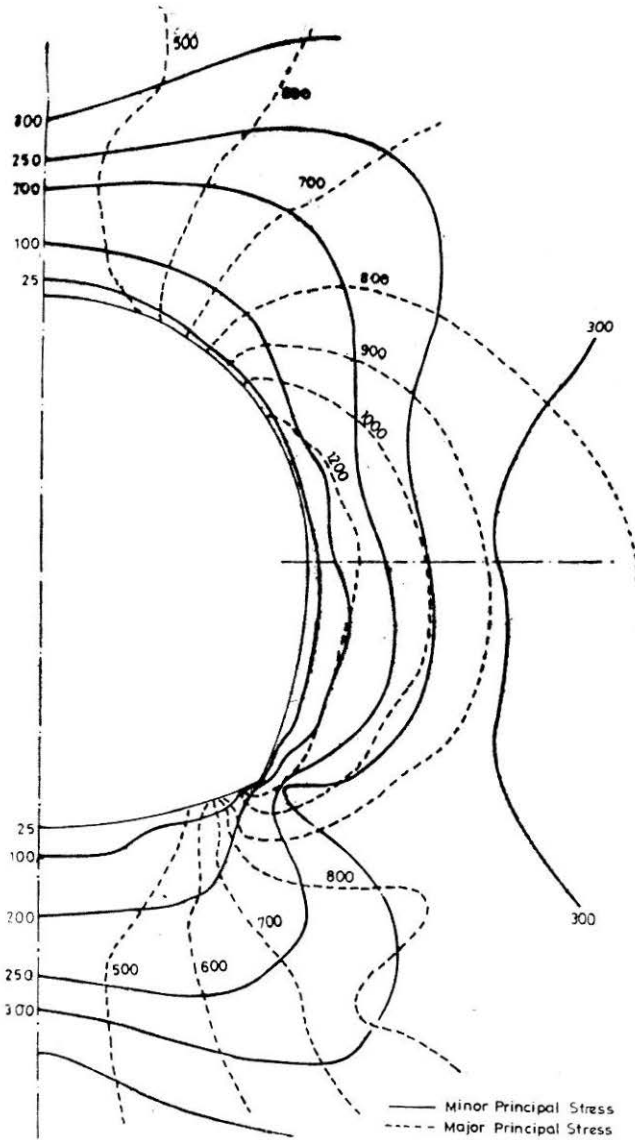


FIGURE 16 Principal Stress Contours—EL Analysis ($K_o = 1.5$)

stage elasto-plastic solution is obtained. The elasto-plastic solution after the second stage excavation does not converge.

In Table 3 are presented the displacements and stresses obtained for case 1ST and case 2ST for some typical locations near the tunnel boundary.

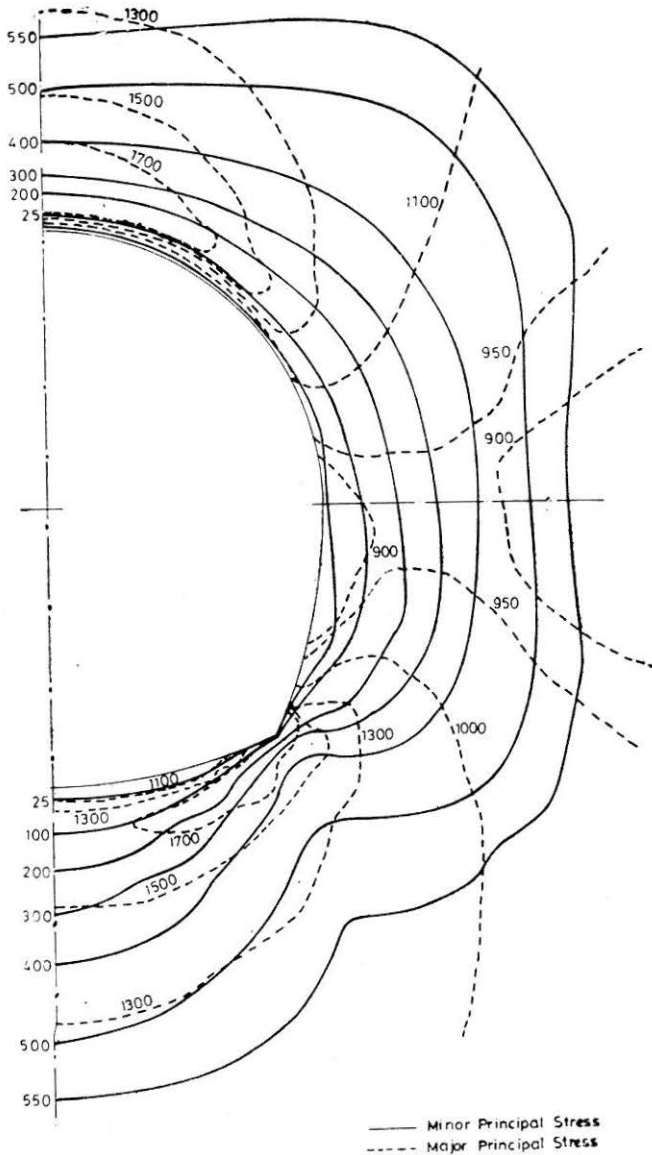


FIGURE 17 Principal Stress Contours—EP Analysis ($K_o = 1.5$)

Conclusions

From the study carried out for elastic and elasto-plastic analyses of horse-shoe shaped tunnel excavated in single and two stages for three insitu stress ratios, following conclusions are drawn.

Considering the displacements at the tunnel boundary, in case of single stage excavation, maximum difference observed between elasto-plastic and

TABLE 3
Stresses and Displacements Near Tunnel Boundary ($K_0 = 1.5$)

Location	Single stage excavation			Two stage excavation		Remarks
	EL	EP	Percentage difference between EP and EL	EP	Percentage difference between two stage and single stage excavation	
Resultant displacement $\times 10^{-3}$ m	1	1.555	1.654	6.30	2.556	54.57
	2	1.696	1.781	5.03	5.353	200.45
	3	1.628	1.719	5.61	12.320	616.38
	4	1.376	1.583	14.97	2.298	45.22
	5	0.886	1.842	107.71	1.852	0.50
Minor principal stress t/m^2	1	57.0	24.67	111.16	24.8	0.70
	2	32.4	27.9	16.09	22.5	-19.11
	3	-21.3	8.7	140.85	-73.0	Large
	4	73.8	47.7	54.66	48.4	1.37
Major principal stress t/m^2	1	2225.6	1098.2	102.65	1099.7	0.33
	2	1256.0	1115.0	12.64	1038.8	7.33
	3	906.0	857.60	5.64	310.0	-63.85
	4	2019.7	1327.4	52.11	1315.5	0.90

EL—elastic analysis

EP—elasto-plastic analysis

elastic analysis is for $K_0 = 1.5$ and it is in the crown portion of the tunnel. Further, in the case of elasto-plastic analysis, for this particular set of properties, the displacements near the tunnel boundary tend to be comparatively uniform all around the tunnel.

A comparison of the displacements for elasto-plastic analysis for single and two stage excavations shows that in general, the displacements obtained from two stage excavation are higher and the difference obtained is maximum in case of $K_0 = 1.5$ in the lower half of the tunnel.

A study of displacement paths shows that the magnitude and direction of movement are affected maximum in the side wall portion of the tunnel for all the cases and it is maximum for $K_0 = 1.5$, for two stage excavation scheme.

A comparison of the principal stress contours for the two types of excavation procedures shows that, in general, the side wall portion of the tunnel is affected more for all K_0 values.

It is observed that in case of two stage excavation, the rock is subjected to tensile stresses near the springing of the tunnel.

A similar analysis carried out for circular tunnels has been reported by Srivastava *et al.* (1986). Following common behaviour are noted for both the cases of underground openings :

- (a) For the present material properties and insitu stress states, if more yielding is indicated the effect of sequence of excavation is more and conversely, if no yielding is indicated, sequence of excavation does not have any effect. Because as expected, the final displacements and stresses are independent of the sequence of excavation in elastic analysis and very much dependent on the sequence of excavation in elasto-plastic analysis.
- (b) It has been found that the sequence of excavation can result in large reversal of stresses and in the direction of movement of the points around the tunnel.
- (c) In case of elastic analysis, displacements are very much a function of insitu stress ratio and the difference in displacements between any two points is more for stress ratios other than 1. In case of elasto-plastic analysis, the displacement distribution tends to be comparatively uniform (for K_0 values not differing much from 1) and the difference in displacements between any two points is comparatively less as compared to elastic analysis.

From a comparison of yielding, displacements and stresses, in case of circular and horse-shoe tunnels for the properties used, it is concluded that

- (i) for insitu stress ratio (K_0) equal to or greater than 1, in case of circular shape of tunnel, less yielding and displacements are obtained as compared to horse-shoe shaped tunnel;
- (ii) for K_0 less than one the reverse trend is observed.

From this it may be concluded that for K_0 equal to or greater than 1, circular shape appears to be better and for K_0 less than 1, horse-shoe shape seems to be better suited.

For the two shapes of tunnels viz. circular and horse-shoe, a comparison of single and two stage excavations shows that single stage excavation should be preferably carried out because in multiple stage excavation, the media is likely to be subjected to tensile stresses also, and the portions which have been excavated in previous stages are subjected to increasing stresses (because of stress redistribution) and hence larger displacements occur in the excavated portion of the tunnel. Moreover, uniformity of displacements and stresses is also lost. This may create difficulties in the choice and provision of support structures.

References

- CHANDRASEKARAN, V.S. and KING, G.J.W. (1974): "Simulation of Excavation Using Finite Elements", *Journal of Geotech. Engg. Div., ASCE*, 100 : 1087-1089.
- HOEK, E. and BROWN, E.T. (1980): "*Underground Excavations in Rock*", Institution of Mining and Metallurgy, London.
- SRIVASTAVA, R.K., SHARMA, K.G. and VARADARAJAN, A. (1986): "Elasto-Plastic Finite Element Analysis of Circular Tunnels", *Indian Geotechnical Journal*, 16 : 295-316.
- ZIENKIEWICZ, O.C. and CORMEAU, I.C. (1974): "Viscoplasticity, Plasticity and Creep in Elastic Solids: A Unified Numerical Solution Approach", *Int. J. Num. Meth. Engg.*, 8 : 821-845.